Title
Physics Requirements on Hadronic Calorimeters at the LHC and SSC

Author
Hearty, C.

Publication Date
1992-10-01

LBL-33102
UC-414

Lawrence Berkeley Laboratory
UNIVERSITY OF CALIFORNIA

Physics Division

Presented at the Third International Conference on Calorimetry in High Energy Physics, Corpus Christi, TX, September 29–October 2, 1992, and to be published in the Proceedings

Physics Requirements on Hadronic Calorimeters at the LHC and SSC

C. Hearty

October 1992

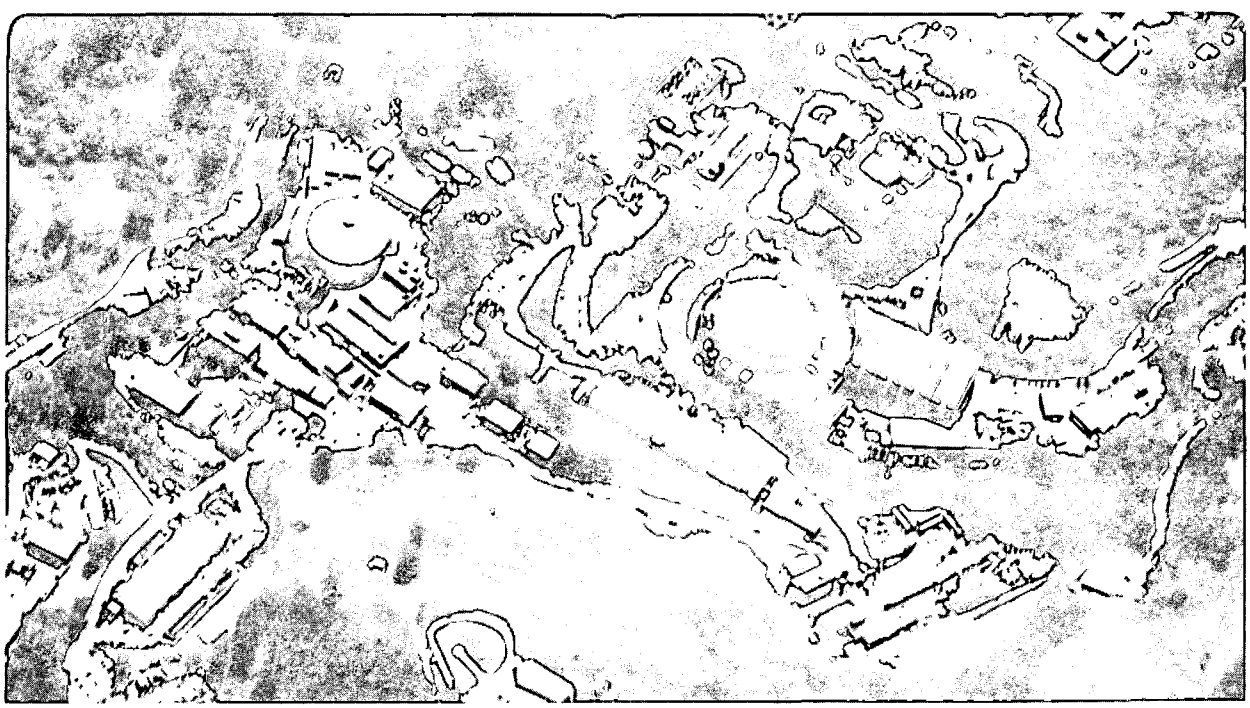

Prepared for the U.S. Department of Energy under Contract Number DE-AC03-76SF00098

DISCLAIMER

PHYSICS REQUIREMENTS ON HADRONIC CALORIMETERS AT THE LHC AND SSC*

CHRISTOPHER HEARTY
Lawrence Berkeley Laboratory
Berkeley, CA 94720

ABSTRACT

The physics goals of hadronic calorimeters at the SSC and LHC are studied to derive requirements on resolution, coverage, segmentation, noise, speed and depth.

Introduction

The hadronic calorimeter measures the energy, position and time of single hadrons, jets and missing-E_t. Examples of physics processes where is it used include tau decays (single hadrons), mass measurements of W's and Z's (or Z''s) through their jet decays; searches for quark substructure (jet cross sections); heavy Higgs decays to two Z's, followed by a decay of one Z to neutrinos; and the detection of supersymmetric particles. The following sections will discuss the specifics of these processes as they relate to establishing requirements on the hadronic calorimeter performance.

Although the emphasis here will be on the physics requirements, the calorimeter design is also driven by a number of other considerations, such as impact on other systems and cost. The impact on other systems will be explicitly discussed when it is one of the primary concerns in determining the requirement. Cost, on the other hand, is not generally mentioned, but it is always a consideration. The purpose of deriving a minimum requirement is not only to ensure that the physics goals of the experiment will be satisfied, but that they will be satisfied at the lowest possible cost.

Absorber Depth

The depth of the calorimeter is driven by the need to reduce leakage (and loss of resolution) and the need to reduce hadronic debris in the muon system.

The most energetic objects observable at the SSC will be high energy jets. Figure 1 shows the mass resolution for 10 TeV dijets as a function of total absorber depth.[1] The jets have been formed from single particle test beam data. Approximately 10λ is sufficient to measure the jets without substantial degradation. The

* This work was supported in part by the Director, Office of Energy Research, Office of High Energy and Nuclear Physics, Division of High Energy Physics of the U. S. Department of Energy under Contract Number DE-AC03-76SF00098.

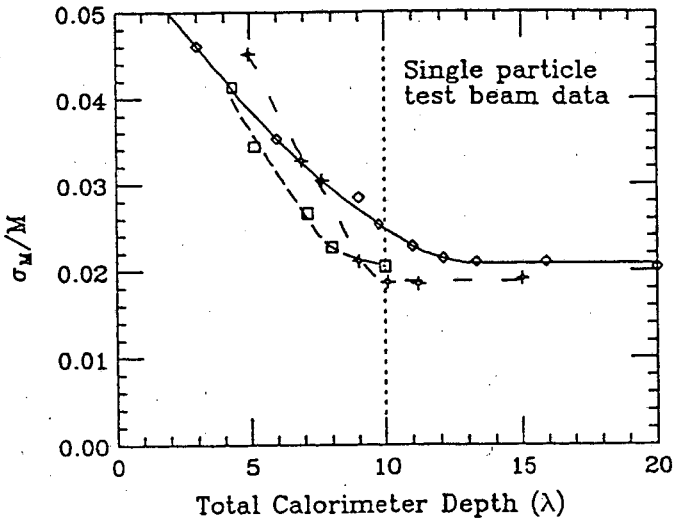

Figure 1. Mass resolution for 10 TeV dijets as a function of total calorimeter depth. The jet response is derived from single particle test beam measurements. The different curves correspond to different data sets.

depth requirement increases logarithmically with energy; since energies are on average higher in the endcap, somewhat greater depth is required there.

The occupancy of the muon system has contributions from prompt muons, muons from pion and kaon decays, and calorimeter leakage. The calorimeter thickness requirement can be established by requiring that the leakage and decay contributions be comparable. The rate of decays is determined by the size of the tracking volume, so the amount of absorber needed is detector dependent. For SDC (170 cm tracking radius), 9λ is sufficient, while for GEM (75 cm radius), 12λ is needed.[2] Of course, the absolute rate will be higher for SDC.

On the basis of this criteria, the longer decay path in the endcap region would imply that less absorber is needed. However, a particular choice for the muon system technology may be matched to the rate expected in the barrel. To achieve the same rate in the endcap requires additional material to range out low energy muons; GEM estimates that 14λ is sufficient.

Absorber Material

The choice of the material used as the absorber influences the resolution, compensation, mechanical structure, calorimeter size, muon multiple scattering, albedo neutron rates, flux return and magnetic field uniformity, and the calorimeter cost. The optimization depends entirely on the design of the rest of the detector and on the priorities of the collaboration.

Angular Coverage

Calorimeter coverage over a large solid angle is essential to the accurate measurement of missing transverse energy. The missing-E_t spectrum due to neutrinos from heavy quark decays in jets sets the scale for the coverage needed. Figure 2 is a plot, for various degrees of coverage, of the ratio of the total missing-E_t cross section to that from neutrinos. For the cross section to be dominated by neutrinos in the region of physics interest (missing-$E_t \geq 100$ GeV), coverage must extend at least to jets with axes at $\eta \leq 5$.[3]

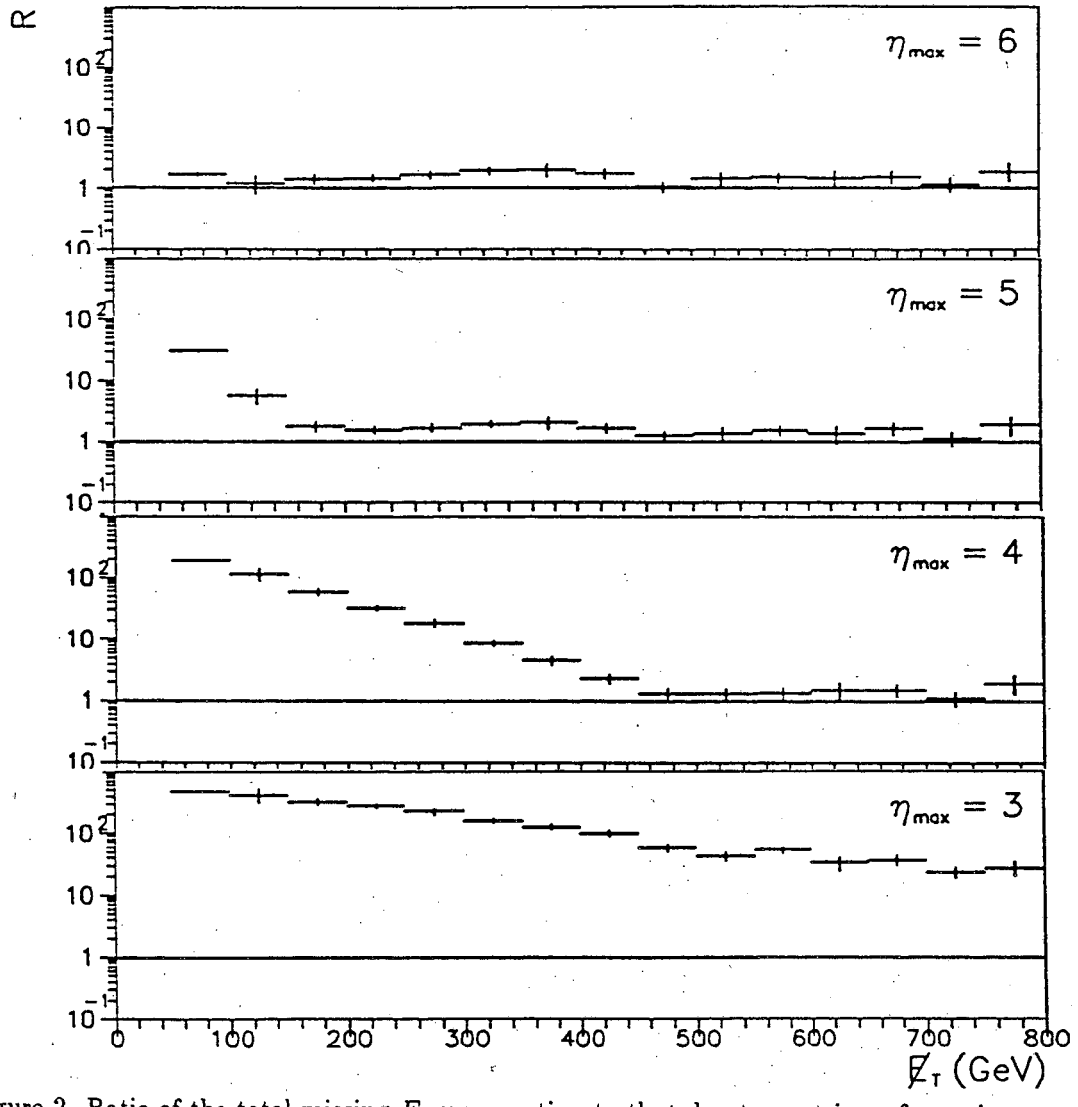

Figure 2. Ratio of the total missing-E_t cross section to that due to neutrinos, for various η_{max}.

A particular physics analysis that relies on missing-E_t is a search for the supersymmetric partner of the gluon, the gluino.[4] The signature for gluino production

is missing-E_t with multiple jets. The background to this process due to neutrinos and jet leakage is significantly larger than the signal, even when coverage extends to $\eta = 5$. The background is topologically different than the signal, however, in that the missing-E_t is colinear with a jet. A cut requiring that the missing-E_t be separated by at least 40° in phi from a jet substantially reduces the background (Fig. 3a). Reducing the calorimeter coverage produces additional background due to jets lost in the beamhole, which is not affected by the phi cut (Fig. 3b).

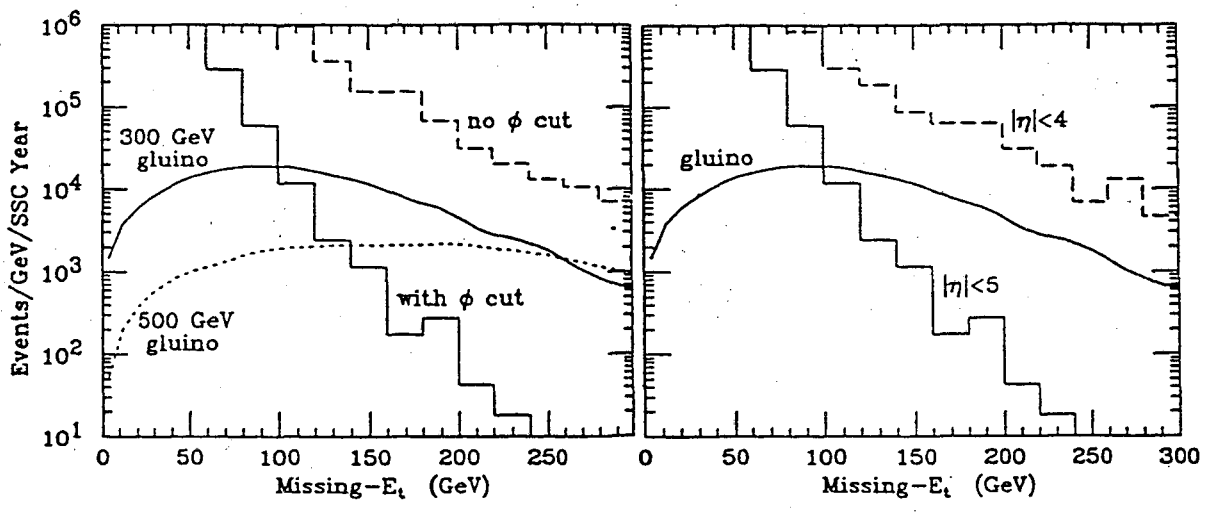

Figure 3. Multijet events per SSC year as a function of missing-E_t. Solid curve is gluino signal. (a) Dashed histogram is background without topology cut, solid histogram is with cut, for jet coverage to $|\eta| = 5$. (b) Backgrounds, with phi cut, for coverage to $|\eta| = 4$ and $|\eta| = 5$.

Forward Calorimetry

The transverse energy resolution requirement on the forward calorimeter is modest: $\sigma_{E_t}/E_t \lesssim 0.1$ is sufficient to ensure that its contribution to the missing-E_t spectrum is negligible at high missing-E_t. The lateral segmentation of 0.2 is sufficient to permit a cut on the angle between the jet and the missing-E_t.

The calorimeter must extend beyond $\eta = 5$ to measure jets at $\eta = 5$. The amount depends on the absorber density and on the distance from the interaction point to the forward calorimeter. Figure 4 shows the transverse energy resolution for single pions as a function of η for a tungsten-liquid argon calorimeter with an inner radius at $\eta = 5.4$, 5.8 or 6.1.[5] Coverage to $\eta = 5.8$ satisfies the requirement on E_t resolution.

The greatest challenge facing the forward calorimeter is not the E_t or position resolution requirements, but extremely high radiation doses. The operation and survival of the device under these conditions may be very challenging. Note that radiation damage may also be a concern for the hadron calorimeter in the endcap, near $\eta = 3$.

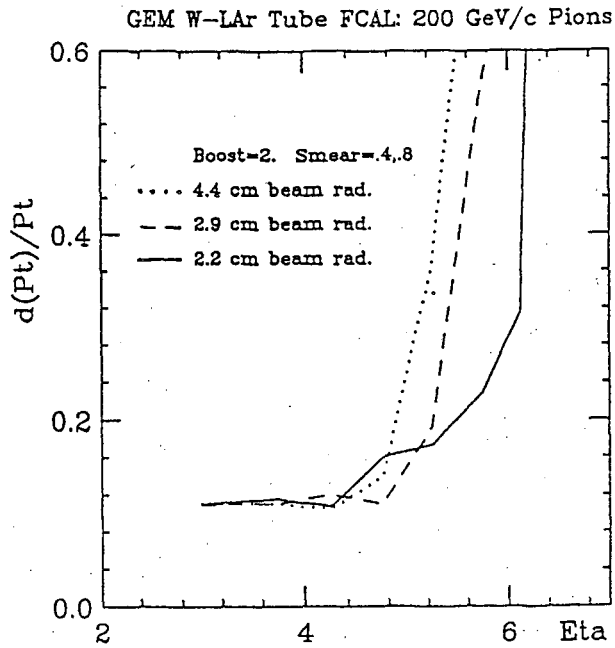

Figure 4. P_t resolution for single pions as a function of incident eta, for a tungsten-liquid argon forward calorimeter with inner radius at $\eta = 6.1$ (solid), 5.8 (dashed), and 5.4 (dotted).

Hermeticity

Missing-E_t will also be generated by gaps in the coverage within the fiducial volume, such as the cracks between calorimeter modules. Figures 5a and b show the missing-E_t generated in 400 GeV E_t jets due to non-interacting particles in two different designs. The first has a projective crack in HAD2 that is displaced in phi from the cracks in the EM and HAD1 modules, while the second has a full depth projective crack. Figure 5c shows, for comparison, the E_t spectrum due to neutrinos. The projective crack in Fig. 5b, which covers approximately 2% of the solid angle, is unacceptable because the missing-E_t is greater than that due to neutrinos. The acceptable upper limit on cracks and gaps is approximately 1% of the solid angle.

Speed, Noise and Pileup

These three quantities are related: a faster calorimeter will observe less pileup, but—at least for liquid ionizing calorimeters—will have larger electronic noise. The optimal integration time depends on the luminosity. LHC detectors must be designed for shorter integration times and must deal with greater pileup than those at the SSC. For hadronic calorimetry, noise is primarily an issue of electron and photon identification efficiency. Noise enters into the Had/EM and isolation cuts.

In CDF, electrons are required to satisfy Had/EM < 0.05 in a region 0.3×0.3 in eta and phi, corresponding to 500 MeV for a 10 GeV electron. At higher luminosity,

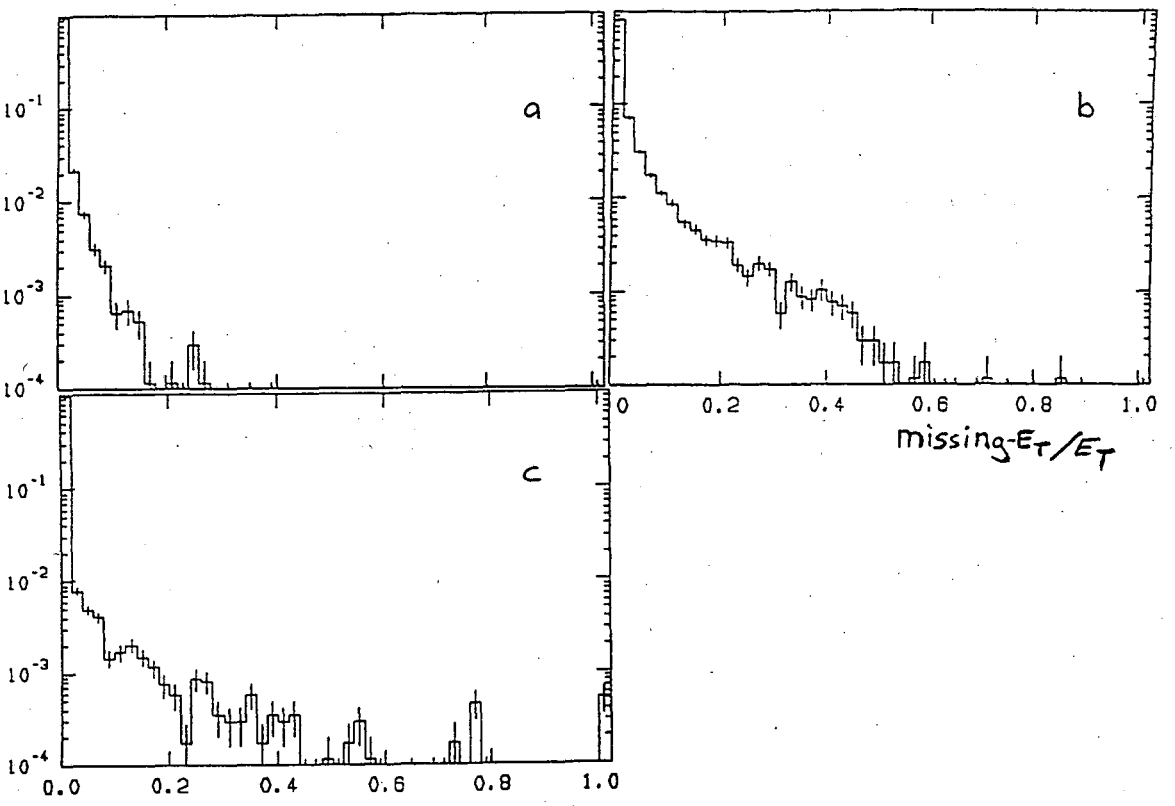

Figure 5. Fraction of energy of 400 GeV jets lost by leakage (averaged over all phi): (a) dogleg hadronic crack; (b) projective crack through full calorimeter. (c) Fraction carried by neutrinos.

the region could be reduced only slightly, since it is intended to tag the debris from a hadronic shower starting in the EM section. A requirement of < 1.0 GeV in 0.2×0.2 appears reasonable.

Isolation is not really electron identification, but rather a topology cut intended to select the desired class of electrons. A tight cut on excess energy surrounding the electron is particularly needed to reject electrons from B hadron decays. Figure 6 shows the excess E_t in a cone of radius 0.3 around electrons from $H \rightarrow ZZ$ and from three backgrounds. A cut of 5–10 GeV is desirable, indicating that the noise in this cone should be less than 5 GeV. (This requirement is on the combined EM and HAD calorimeters, while the requirement in Had/EM is based on HAD only).

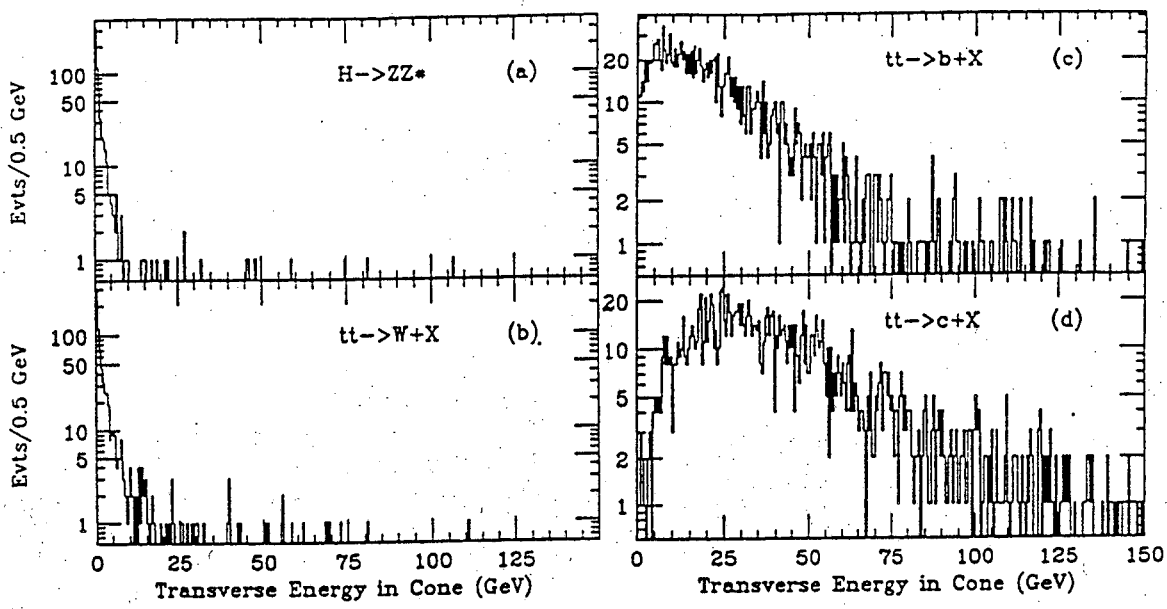

Figure 6. Excess E_t in a cone of radius 0.3 around electrons from $H \rightarrow ZZ$ and three different backgrounds. Calculation is at an SSC luminosity of 10^{33} cm^{-2}sec^{-1}.

Timing Resolution

The calorimeter speed and noise also influence the timing resolution. Timing resolution is largely a trigger issue, since the trigger indicates to the front-end electronics the correct buckets to examine. The requirement, therefore, is that the trigger system be able to correctly "bucket-tag" energy deposits of interest. For the hadronic calorimeter, this corresponds approximately to $\sigma_t < 4$ ns for jets of $E_t \geq 100$ GeV.

Segmentation

Longitudinal Segmentation

The H1 calorimeter has ten depth segments, of which six are in the hadronic calorimeter. This fine segmentation allows the intrinsically noncompensating response to be corrected by software. The result is a substantial improvement in pion resolution: $0.58/\sqrt{E} \oplus 0.063 \rightarrow 0.46/\sqrt{E} \oplus 0.015$.[6] However, it is not clear whether this method works as well for high-pt jets at the LHC and the SSC. In any case, it may be overkill for the LHC and SSC, which have less stringent requirements on resolution.

The last 3λ, if read out separately, can be used to somewhat correct for leakage, or at least, to tag events with substantial leakage (Fig. 7). A thicker calorimeter will benefit less from this segmentation.

Other benefits of longitudinal segmentation are technology dependent. Since most of the energy in contained in the first 5λ (85% for 100 GeV pions), the sampling

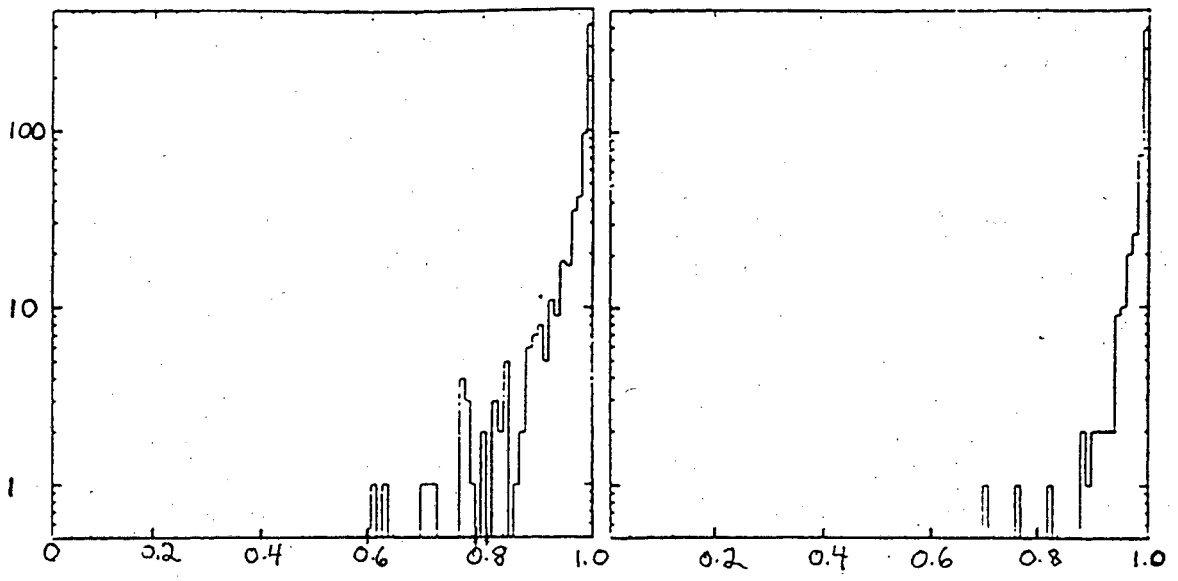

Figure 7. Fraction of the energy of a 450 GeV pion contained in a 10λ calorimeter (test beam data). (a) Without leakage cut; (b) after rejecting events with more than 30% of the energy in Had2.

fraction can be reduced in the remainder, reducing the overall cost. Figure 8 is a plot of the resolution observed for 240 GeV pions incident on a 9.5λ thick calorimeter divided into EM, HAD1 and HAD2 compartments, for various HAD2 thicknesses and sampling fractions.[7] Reducing the sampling fraction by a factor of two for the last 5λ has only a small impact on the resolution.

Finally, liquid ionizing calorimeters may find it necessary to subdivide the device in order to reduce the capacitance per channel or to provide redundancy (when the preamplifiers are inaccessible).

Lateral Segmentation

The physics most sensitive to the lateral segmentation is the mass measurement of boosted W's decaying into jets, where the jets tend to merge together. The sensitivity to segmentation has been examined by studying the decay of a 1 TeV Higgs boson: $H \rightarrow WW \rightarrow l\nu$ *jet jet*. The event is required to have two narrow jets within a single larger jet. Figure 9 shows the reconstructed mass peaks for various lateral segmentations in the hadronic calorimeter. The mass resolution is plotted as a function of segmentation in Fig. 10. Lateral segmentation coarser than 0.1 results in significantly poorer resolution.

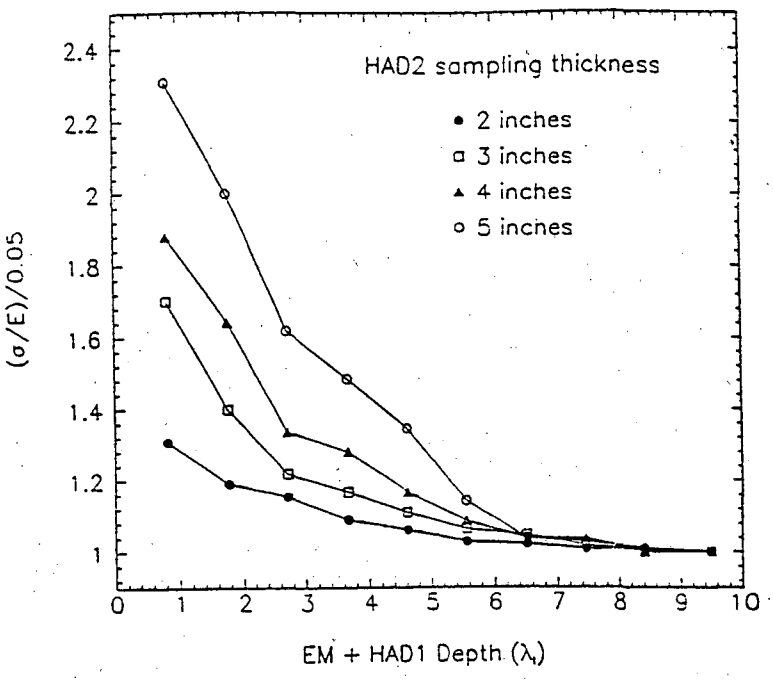

Figure 8. Resolution (σ_E/E) for 240 GeV pions as a function of the EM+HAD1 depth. HAD2 is constructed from various absorber plate thicknesses, and brings the total depth to 9.5λ.

Resolution

Single Particles

Physics at the SSC and LHC will rely much more on jets than on single hadrons, so it is the jet resolution requirements that drive the design. A potential exception, the hadronic decay of taus, has not yet been studied sufficiently.

If the muon system is designed such that the momentum measurement of muons is made outside of the calorimeter, rather than in the central tracker, the energy lost by muons in the form of δ-rays can produce a significant low-end tail. GEM studies indicate that a resolution of $\sim 45\%/\sqrt{E}$ for these energy deposits in the hadron calorimeter is sufficient to provide a meaningful momentum correction.

Jet Resolution

The jet energy resolution has little impact on the measurement of the jet cross section (for compositeness searches, for example).[8] It matters most in mass measurements. Different classes of events are discussed below.

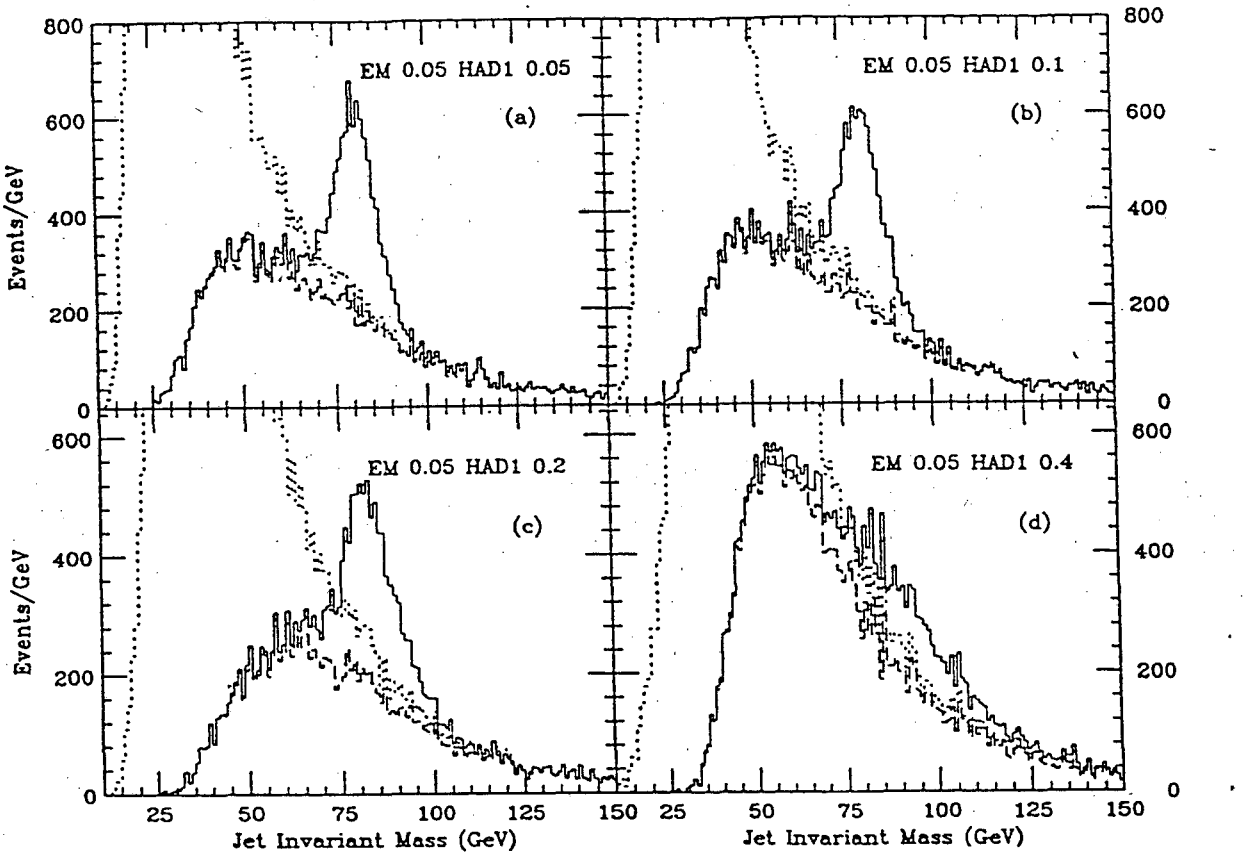

Figure 9. Reconstructed mass from high-pt $W \rightarrow$ jet jet for various HAD1 lateral segmentation. The dotted curve shows the shape of the two-jet background before requiring two narrow jets within a single cone. The solid and dotdash curves are after applying this cut. The true background rate is approximately thirty times the level shown here.

Low-pt Jets

Low-pt W's and Z's decay to low-pt jets. In this case, clustering algorithms, fluctuations in and out of the jet cone, magnetic field effects, and pileup dominate the mass resolution. Figure 11 shows the Z mass resolution observed under a variety of conditions. The difference in resolution between a perfect calorimeter (second case) and a nonlinear calorimeter with resolution $70\%/\sqrt{E} \oplus 4\%$ (last point) is small. It should be noted, however, that the tracker could help correct some of these effects. This figure does not include of pileup, which is an important contribution to the resolution, particularly at the LHC. Figure 12 compares the mass resolution for low-pt Z's for a perfect calorimeter with and without pileup at a luminosity of 10^{34} cm^{-2}sec^{-1}.

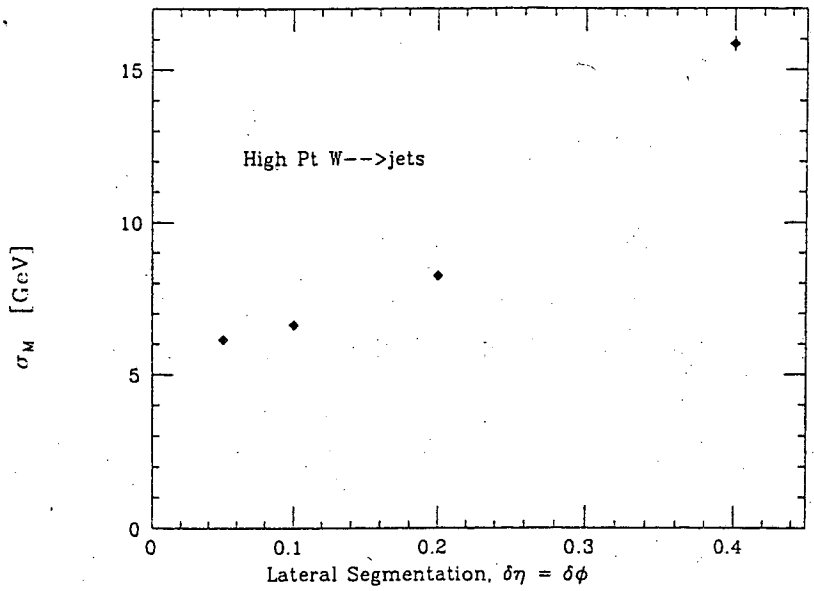

Figure 10. Mass resolution for high-Pt W's as a function of lateral segmentation in the hadronic calorimeter. EM segmentation is 0.05×0.05.

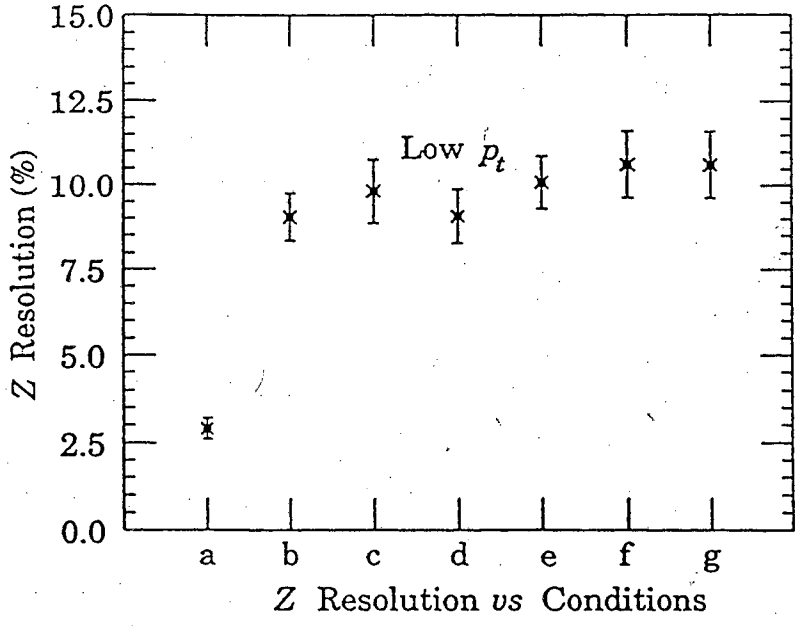

Figure 11. Mass Resolution for low-p_t Z's decaying to jets under a variety of conditions. (a) perfect detector, (b) include shower shape, but perfect energy resolution, (c)–(g) hadron energy resolution $0.30/\sqrt{E} \oplus 0.02$ (linear) $\rightarrow 0.70/\sqrt{E} \oplus 0.04$ (nonlinear).

High-pt Jets/Low Mass Object.

A high-pt, low mass object (a boosted Z, for example) will decay into high-pt jets that tend to merge together. As discussed earlier, lateral segmentation is the most

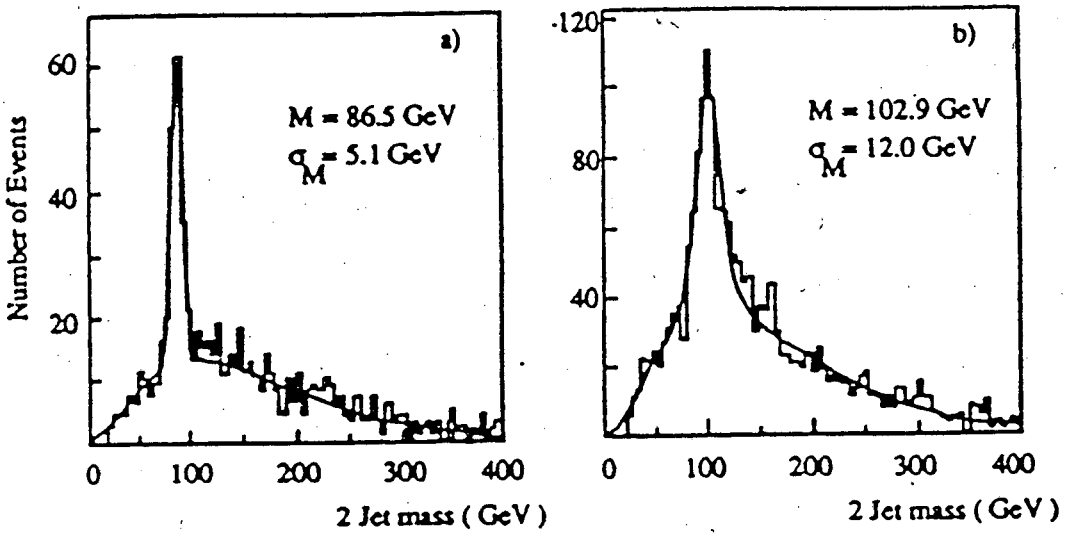

Figure 12. Two jet mass resolution for low p_t $Z \rightarrow$ jet jet with an ideal calorimeter at the LHC. (a) no pileup; (b) with pileup for 10^{34} cm^{-2}sec^{-1}.

significant parameter under these circumstances. Table 1 summarizes the observed boosted-Z mass resolution for various calorimeter energy resolutions. The middle case—single hadron resolution of $0.67/\sqrt{E} \oplus 0.06$—corresponds to a jet resolution of $0.63/\sqrt{E} \oplus 0.02$, including the effect of the e/π nonlinearity. This resolution appears to be adequate.

Table 1. Mass resolution for high-pt W's with segmentation of 0.05 in EM, 0.10 in HAD. Resolutions do not include pileup.

Single Hadron Resolution	Mass Resolution (σ_M)
$0.40/\sqrt{E_t} \oplus 0.02$	4.54 ± 0.11 GeV
$0.67/\sqrt{E_t} \oplus 0.06$	5.31 ± 0.13 GeV
$1.00/\sqrt{E_t} \oplus 0.10$	6.17 ± 0.14 GeV

High-pt Jets/High Mass Object

A massive Z' will decay to high pt jets that do not tend to merge together. Table 2 summarizes a GEM study of the mass resolution for a 1 TeV Z'.[9] The third line, $\sigma_M/M = 0.029$, includes detector independent effects and corresponds to very good jet resolution: approximately $0.50/\sqrt{E}$ with no constant term. In this calculation, the 2% hadron constant term is reduced by approximately the square-root of the number of particles in the jet. The last line adds a 2% jet resolution constant term, which degrades the mass resolution by 20%. Again, this appears to be acceptable.

It is worth noting that the detection and mass measurement of a heavy gauge boson will be very much easier with leptons, which do not have the large QCD backgrounds associated with the hadronic channel.

Table 2. Mass resolution for a 1 TeV Z' decaying to jets for a variety of cases.

Case	Mass Resolution (σ_M/M)
Perfect Resolution, GEM segmentation, clustering	0.028
$0.50/\sqrt{E} \oplus 0.02$	0.028
Transverse shower spreading	0.029
Additional 2% jet constant term	0.035

Jet Linearity

The correct calibration of the jet energy is needed to correctly measure the mass of objects decaying to jets. It is equally important in measurements of the jet cross section. An excess of jets at high-pt is a signature for compositeness, but can also result from the promotion, via a nonlinear jet response, of lower-pt jets. A study by the Eagle collaboration indicates that a jet response that is linear to 500 GeV, then deviates from linearity until it is nonlinear by 4% for 4 TeV jets, will mask a compositeness signal corresponding to a 15 TeV contact term (Fig. 13).[8] A similar study by SDC indicates that a nonlinearity of 1% per TeV above 2 TeV (*i.e.*, a nonlinearity of 1% at 3 TeV, 2% at 4 TeV) will mask a 25 TeV contact term.[10] Combining these two studies, the nonlinearity be less than 1% per TeV above 1 TeV. This is a limit on the error after corrections have been applied. The shape of the linearity curve, except at the highest pt, can be measured with γ-jet events, and may also be extracted from W and Z mass measurements. The shape can also be predicted by convoluting single particle responses, measured in test beams, with fragmentation models. The comparison will provide confidence in simulations of calorimeter response.

The limit on the error in jet linearity translates into a relatively loose requirement on the single hadron calibration. As shown in Fig. 14, an error in π/e of 5% per TeV above 100 GeV corresponds to an error in jet linearity of approximately 0.3% per TeV above 1 TeV.

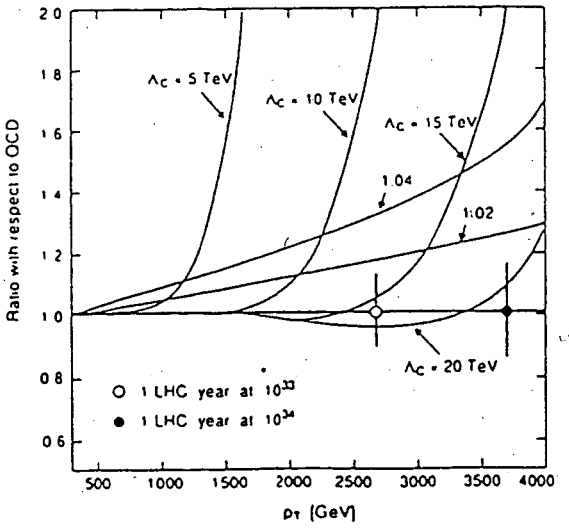

Figure 13. Ratio of observed jet cross section to QCD cross section for various compositeness contact terms. The dashed lines indicate the impact of residual nonlinearities in the pion response. (The value is the nonlinearity at 4 TeV). The black and open circles are the statistical sensitivity for $10^4 pb^{-1}$ and $10^5 pb^{-1}$.

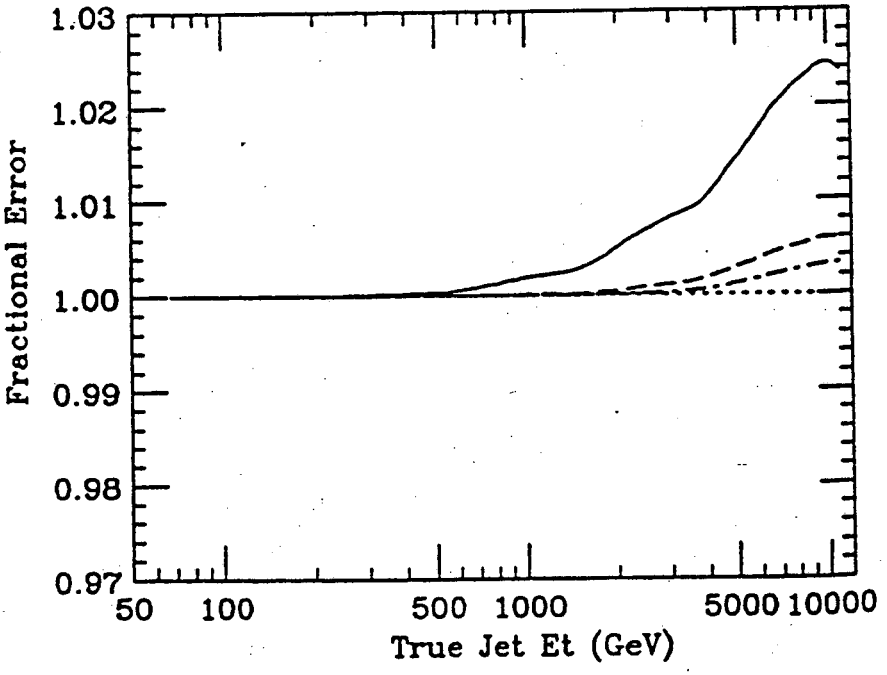

Figure 14. Deviations from linearity for jets induced by systematic errors in the knowledge of the single particle π/e. The solid line is for perfect calibration to 100 GeV, with a 5% per TeV extrapolation error for higher energies. The dashed and dot-dashed curves correspond to an extrapolation error of 2% per TeV and perfect calibrations to 500 and 1000 GeV respectively.

Compensation

The physics goals of the LHC and the SSC emphasize good EM calorimetry,

which for almost all reasonable designs is not only noncompensating, but also will have a different response to electrons and pions than the hadron calorimeter. As a result of this mismatch, $\pi/e \neq 1$ for the complete calorimeter, and the single pion resolution constant term is worse than would be expected for the hadron calorimeter alone. This effect is illustrated by a Calor89 calculation of the pion resolution of a 10λ thick hadron calorimeter constructed from 21 mm lead plates alternating with 4 mm scintillator.[11] The device is nearly compensating, with pion resolution $\sigma_E/E = 0.64/\sqrt{E}$. However, when an EM section consisting of 36 layers of 3.25 mm lead precedes this hadron calorimeter, the resolution becomes $\sigma_E/E = 0.57/\sqrt{E} \oplus 0.04$. The 4% constant term arises because the observed energy depends on the energy fraction deposited in the EM compartment (Fig. 15).

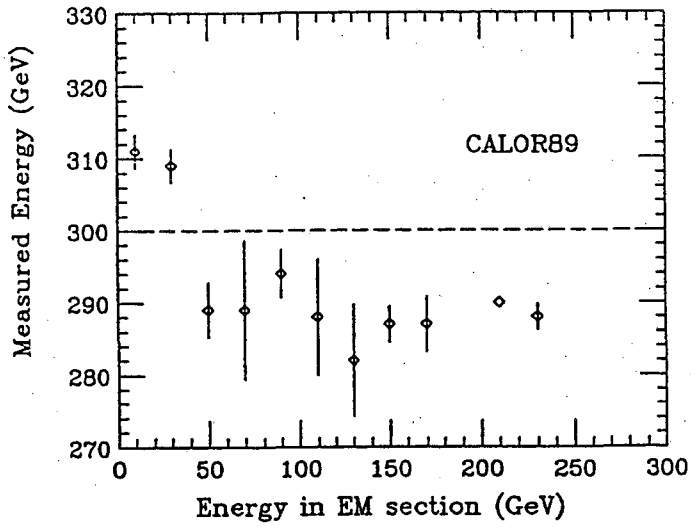

Figure 15. Average energy measured for 300 GeV pions vs the energy in the EM compartment.

Calculations using parameterized showers suggest that a compensating hadronic calorimeter will simplify understanding the jet response, even when the EM calorimeter is noncompensating.[12] Specifically, that the true jet energy depends linearly on the signal in the EM compartment and the total observed energy, and that the slope of this relationship can be extracted in test beams. However, it is not clear that the parameterized shower simulation is reliable enough to support the conclusions.

In general, the signals measured in each longitudinal compartment can be added with arbitrary relative weight to produce the best estimate of the energy. The H1 method of optimizing pion resolution is an example. The difficulty with this method is that it requires a large event sample for training. This is possible for pions, but more difficult for jets. Furthermore, it requires fine longitudinal segmentation, at a cost that may not be justified by the resolution requirements discussed earlier.

Looking at weighting in simpler terms, the relative weight of signals between EM and HAD is an arbitrary constant. Jet performance—rather than single pion resolution, for example—is the quantity to be optimized. In practice, this means weighting the hadron calorimeter to achieve $\pi/e \sim 1$ over a wide energy range. This is illustrated by another Calor89 calculation of the pion and jet responses of a calorimeter consisting of EM: 36 × (3.2mm pb + 4mm scintillator); HAD1: 32 × (2.5cm iron + 2.5mm scintillator); and HAD2: 12 × (5.1cm iron + 2.5mm scintillator). The e/h of the hadron calorimeter is approximately 1.5. Two different weighting methods give significantly different jet resolutions and linearities. The first method, which nearly optimizes pion energy resolution, gives $\pi/e = 1$ at $E = \infty$. The second method weights the hadron calorimeter to give $\pi/e = 1$ at $E = 300$ GeV. The pion and jet resolutions are $0.57/\sqrt{E} \oplus 0.048$ and $0.55/\sqrt{E} \oplus 0.030$ for the first method, and $0.63/\sqrt{E} \oplus 0.053$ and $0.56/\sqrt{E} \oplus 0.016$ for the second. Figure 16 shows the pion and jet linearities. The second method (finite-energy calibration), substantially reduces the impact of the noncompensating calorimeter. Note that the jet resolution with this method satisfies the requirement specified above, indicating that even a noticeably noncompensating calorimeter can satisfy the physics goals for the SSC and the LHC.

Summary

The requirements on hadron calorimeters at the SSC and the LHC are summarized below.

Item	Requirement
Absorber depth	10λ active, 10–12 total; more in EC
Angular coverage	measure jets to $\eta = 5$
Forward Calorimeter	$\delta p_t/p_t \approx 0.1$; 0.2 segmentation
Hermeticity	cracks, holes $< 1\%$
noise/pileup	< 5 GeV 0.3 cone (all); < 1 GeV 0.2×0.2 (had)
long. segmentation	useful to tag leakage, reduce cost
lateral segmentation	$\leq 0.1 \times 0.1$
jet resolution	$\sim 0.60/\sqrt{E_t} \oplus 0.02$
jet nonlinearity	$< 1\%$/TeV above 1 TeV

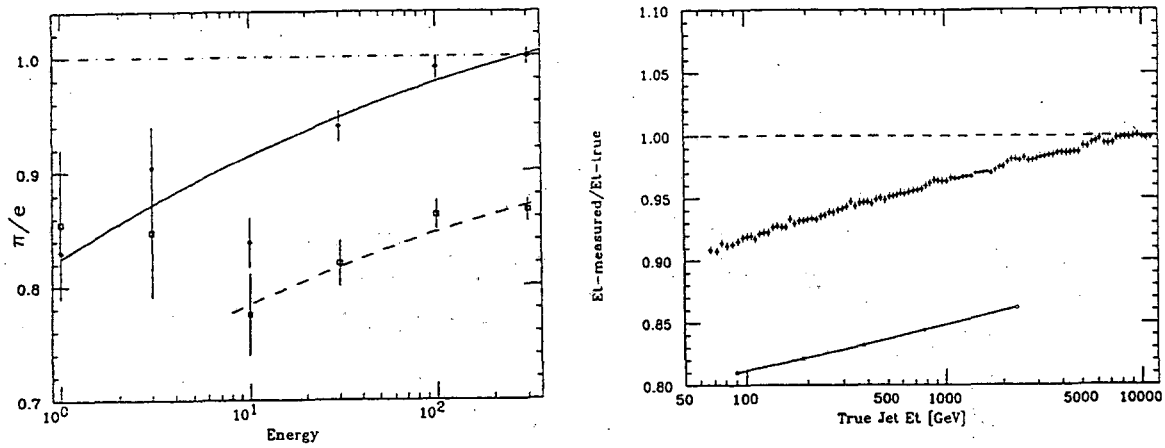

Figure 16. Linearity for (a) pions, and (b) jets, for two different hadronic weighting schemes. The upper line in both cases corresponds to weighting the hadron calorimeter such that $\pi/e = 1$ at 300 GeV; the lower line corresponds to $\pi/e = 1$ at $E = \infty$, and optimizes the single pion energy resolution.

REFERENCES

1. D. Green, *et al.*, *Depth Requirements in SSC Calorimeters*, Fermilab-FN-570, August 1991.
2. R. McNeil, *How Thick Should the GEM Barrel Calorimeter be?*, GEM TN-92-68 Rev. A, March 1992.
3. F. E. Paige, A. V. Vanyashin, *Effects of Limited Calorimeter Coverage on Missing-E_t*, GEM TN-92-70, March 1992.
4. *Solenoidal Detector Collaboration Technical Design Report* (SSCL-SR-1215, April 1992), Sec. 3.4.
5. M. A. Shupe, *these Proceedings.*
6. H1 Calorimeter Group, *Results from a Test of a Pb-Fe Liquid Argon Calorimeter*, DESY-89-022, February 1989.
7. A. Beretvas, *et al.*, *Beam Tests of Composite Calorimeter Configurations from Reconfigurable-Stack Calorimeter*, to be submitted to NIM, June 1992.
8. L. Poggioli, *Proceedings of the Second International Conference on Calorimetry in High Energy Physics* ed. A. Ereditato, (World Scientific, 1992), p. 353.
9. *GEM Letter of Intent*, Sec. 3.5, November 1991.
10. *SDC Expression of Interest*, Sec. 3.6, May 1990.
11. The author wishes to thank Tom Handler for generating this Calor89 data.
12. H. P. Paar, R. Wigmans, *Jet-Energy Measurements with a Noncompensating Calorimeter System*, GEM TN-92-67, February 1992.

LAWRENCE BERKELEY LABORATORY
UNIVERSITY OF CALIFORNIA
TECHNICAL INFORMATION DEPARTMENT
BERKELEY, CALIFORNIA 94720